Back-to-back competitive learning mechanism for fuzzy logic based supervisory control system of hybrid electric vehicles

Li, Ji; Zhou, Quan; Williams, Huw; Xu, Hongming

DOI:
10.1109/TIE.2019.2946571

Back-to-back Competitive Learning Mechanism for Fuzzy Logic based Supervisory Control System of Hybrid Electric Vehicles

Ji Li, *Member, IEEE,* Quan Zhou*, Member, IEEE,* Huw Williams, and Hongming Xu*

***Abstract*—This paper proposes a novel back-to-back competitive learning mechanism (BCLM) for a fuzzy logic (FL) supervisory control system for hybrid electric vehicles (HEVs). This mechanism allows continuous competition between two fuzzy logic controllers during real-world driving. The leading controller will have the regulatory function of the supervisory control system. Firstly, the configuration of the HEV model and its FL-based control system are analysed. Secondly, the algorithm of chaos-enhanced accelerated particle swarm optimization (CAPSO) is developed for back-to-back learning of the membership function. Thirdly, based on fuel-prioritized cost functions, the regulation of competitive assessment is designed to select a controller with a better fuel economy. Finally, the competitive performance of using the CAPSO algorithm is contrasted with other swarm-based methods and the BCLM-driven control system is validated by a hardware-in-the-loop test. The results demonstrate that the BCLM control system significantly reduces fuel consumption, at least 9% from charge sustaining and charge depleting based, and at least 7% from conventional FL-based systems.**

***Index Terms*—Competitive learning; fuzzy logic control; hybrid electric vehicles; online energy management; parallel computing; particle swarm optimization.**

I. Introduction

The increase in emissions that is associated with transportation growth is posing a severe challenge to CO_2 mitigation and urban air quality improvement [1]. Conventional vehicles propelled by internal combustion engines (ICEs) benefit from the very high energy density of petroleum-based fuels but suffer from low efficiency [2]. As a transitional technology to the full electrification of road vehicles, hybridization offers improved fuel economy and reduced exhaust emissions [3]. Hybridization is expected to play a significant role in the transformation of the automotive industry over the next 2-3 decades [4]. For hybrid electric vehicles (HEVs), developing optimal energy management strategies is critical to achieving the best performance and energy efficiency through power-split control.

The existing energy management of HEVs can be generally classified into heuristic strategies that depend on a set of rules to determine the control action at each time instant, and optimization-based strategies that seek to achieve the best compromise between competing objectives. The heuristic rules are designed in accordance with intuition, human expertise, and/or mathematical models and, usually, without a priori knowledge of customer usage [5]. The fuzzy logic (FL) approach is one of the typical heuristic strategies and it plays an essential role in handling measurement noise and component variability through its adaptive character [6]. This paper elaborates FL-based applications in the automotive industry, to encompass forward information fusion and supervisory energy management.

Forward information fusion is the process of integrating multiple data sources to produce more consistent, accurate, and useful information [7], especially for human component systems like HEVs. Driving style recognition plays an important role in vehicle energy management as well as driving safety [8]. In the work of Zhang and Xiong [9], a hierarchical control strategy is simulated for multiple energy sources, in which a driving pattern recognition method is developed using fuzzy logic controllers (FLCs). Jing et al. [10] proposes a cooperative method for vehicle speed prediction that uses a fuzzy C-mean algorithm with an unsupervised learning process to classify acceleration states. In the work of Filev and Kolmanovsky [11], a fuzzy encoding technology is presented to develop conventional Markov chain models with a continuous range, (also applied in the research of Li et al. [12]). In intelligent transportation systems, FL theory has been used to develop a vehicle detection algorithm for traffic scene interpretation [13]. Milanés et al. [14] builds an intelligent automatic overtaking system using vision for vehicle detection, in which an FLC was developed to emulate how humans overtake.

The supervisory energy management system is responsible for controlling the power flows from the individual sources, while guaranteeing sufficient provision for the traction system's operation [15]. FL-based control systems with good robustness can optimally address this issue (see Refs [16], [17]). Type-2 (probabilistic) FLC has been applied in an electrical chain

Manuscript received April 04, 2019; revised June 26, 2019 and August 15, 2019; accepted September 30, 2019. (*Corresponding author: Hongming Xu*.)

The authors are with the Department of Mechanical Engineering, the University of Birmingham, Birmingham, B15 2TT, U.K. (e-mail: jxl592@bham.ac.uk; q.zhou@pgr.bham.ac.uk; huw.trefor.williams@gmail.com; h.m.xu@bham.ac.uk).

components evaluation vehicle and evaluated by simulation [18] and experiment [19]. The results demonstrated that type-2 FLC can be widely adopted for performing energy management. In the work of Kheirandish et al. [20], a dynamic fuzzy cognitive network is proposed to describe the behaviour of a fuel cell electric bicycle. However, such FL-based systems are established based on human cognition, and their performance is largely limited by empirical knowledge. Tian et al. [21] propose data-driven hierarchical control for online HEV energy management, in which driving data is used to train membership functions in adaptive neuro-fuzzy inference systems working as an online energy management system. In the works of Zhou et al. [23] and Collotta et al. [24], the FL-based control systems are optimized offline using genetic algorithms and particle swarm optimization. These proposed systems still have potential to upgrade to an online version with dynamic fuzzy parameter adaption [24].

Optimization-based control approaches rely on analytical or numerical optimization algorithms. Kolmanovsky [25] describes the development and experimental implementation of game theory for HEV energy management. Game theory, however, requires deep knowledge of the system elements and consequently cannot be extrapolated to other vehicle types [26]. In the work of Liu et al. [27], reinforcement learning techniques are applied to hybrid electric tracked vehicles, wherein a transition probability matrix is learned from a specific driving schedule of the vehicle. The upgrade version, deep reinforcement learning [28], has been employed by Wu et al. [29] to develop a continuous control strategy for hybrid electric buses. However, feasibility and stability of implementing such model-free algorithms into an actual vehicle controller needs to be further investigated and validated. In the research of Ahmadi et al. [30], a genetic algorithm is invoked to accurately adjust control parameters of an FLC, and its result shows that fuel economy and vehicle performance are significantly improved. Dynamic programming as a representative of global optimization algorithms usually depends on a model to provide a provably optimal control strategy by searching all state and control grids exhaustively [9], [31]. However, dynamic programming and genetic algorithms are not applicable to real-time problems since precise future driving information is seldom available in practice [32].

In order to break through these research limitations, this paper proposes a novel back-to-back competitive learning mechanism (BCLM) for synergistic promotion of robustness and efficiency of HEV systems. Relying on parallel computing techniques, this mechanism continuously selects from two competing FLCs that form part of the supervisory control system, during real-world driving. To the best of the authors' knowledge, there are no vehicular applications involved such a parallel control system in the literature. The proposed mechanism is expected to break through the upper limit of heuristic system decision and compensates the lower limit of optimization-based system decision then make two systems complement each other. Firstly, the configuration of the HEV model and its FL-based supervisory control system are analysed and discussed. Secondly, the chaos-enhanced accelerated particle swarm optimization (CAPSO) algorithm is developed for back-to-back learning of the membership function's scalar parameters. Thirdly, based on fuel-prioritized cost functions, the regulation of competitive assessment is designed to select a controller with better fuel economy. Fourthly, the competitive performance of the CAPSO algorithm is contrasted with other swarm-based methods, and the BCLM-driven control system is validated by a hardware-in-the-loop (HiL) test. Finally, the length of observation windows for learning from the backward horizon is studied in this paper and its influence on fuel consumption is investigated.

The configuration of the HEV is presented and its FL-based control system is discussed in section II. The concept of the proposed BCLM is elaborated in section III and its two modules of back-to-back learning and competitive assessment are explained. Section IV describes the generation of test cycles, the human drivers who produced them, and the HiL experimental platform. Section V carries out a comparative study of different control policies, including their computational efficiency, for HEV energy management. Conclusions are summarized in section VI.

II. PROPOSED SOLUTION

A. HEV Configuration

The series-parallel HEV powertrain, which is supervised by the vehicle controller, comprises a gasoline engine, an integrated starter-generator (ISG), a trans-motor and is powered by a combination of fuel and electricity as shown in Fig. 1. The ICE's drive (post transmission) and the trans-motor's drive are combined by coupling them in series so that their speeds are added (forcing equal torques), although as set out in [33] they can be decoupled via the operation of the clutch and the locks. The peak power of the trans-motor is $P_{mot^*} = 75$ kW with 270 Nm maximum torque. The peak power of the gasoline engine is $P_{ICE^*} = 63$ kW with 140 Nm peak torque. The peak power of the ISG is $P_{ISG^*} = 32$ kW. The vehicle data, representing a medium passenger car, was sourced from ADVISOR software. The main parameters of the HEV model are listed in Table 1.

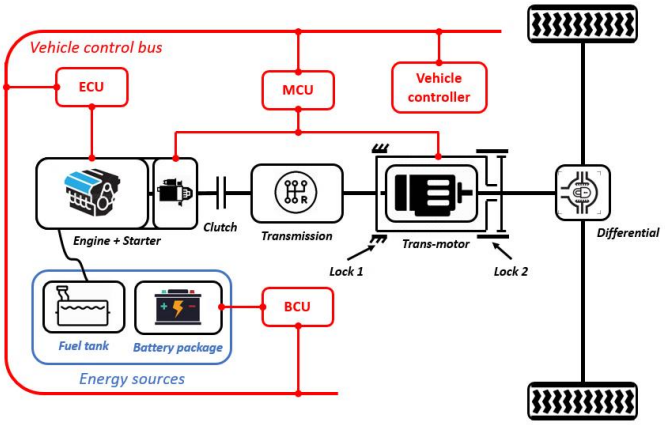

Fig. 1. The architecture of series-parallel HEV powertrain

TABLE 1
MAIN PARAMETERS OF THE HEV MODEL

Symbol	Parameters	Values
M	Gross mass	1,500 kg
A_f	Windward area	2 m^2
R_{wh}	Tire rolling radius	0.3 m

C_d	Air drag coefficient	0.3
i_0	Differential ratio	3.75
i_g	Transmission ratio	3.55/1.96/1.30/0.89/0.71

B. FL-based Supervisory Control System

In order to rationally assign the vehicle's power demand, P_d, which has a corresponding torque demand (measured at the reducer input), T_d, to the three machines, it is paired with the state of charge, SoC, of the battery pack (BP) to make up the input to the FL-based supervisory control system that chooses between the two modes of pure electric traction, $Mode_{EV}$, and FL-based traction, $Mode_{FLC}$, and is expressed as follows:

$$\left.\begin{aligned}(T_{mot}, P_{ice}, P_{gen}) &= Mode_{EV}(P_d, SoC), \quad SoC > 0.5,\\ (n_{mot}, P_{ice}, P_{gen}) &= Mode_{FLC}(P_d, SoC), \quad SoC \le 0.5,\end{aligned}\right\} \tag{1}$$

where: T_{mot} is the trans-motor torque; n_{mot} is the trans-motor speed; P_{ice} is the ICE power; and P_{gen} is the ISG power.

The electric traction system has the capacity to completely satisfy the torque demand, enabling deactivation of the ICE and the ISG in the electric mode. The power distribution in this state is therefore given by

$$(T_{mot}, P_{ice}, P_{gen}) = (T_d, 0, 0). \tag{2}$$

In the fuzzy logic control mode, FLCs are used to perform energy management. This structure supplies power to propel the vehicle while maintaining the BP's SoC between safe limits. The design of the FLCs is described below.

1) Fuzzification

The fuzzy sets with linguistic terms are regulated with standard triangular membership functions (MFs), where the degree of membership is expressed as a function of normalized values in the interval, [0,1]. The values of the MFs in the FLC are set at 3 levels: Low, Medium, and High. These functions fuzzify the crisp inputs.

The power demand may take both positive and negative values and is bounded by the maximum (accelerative) power, P_d^+, and the minimum (powertrain braking) power, P_d^-, which is negative. The "knee point" of the corresponding input, $Input_1$, is not set at the midpoint between the power demand boundaries: it is set via

$$Input_1 = \begin{cases} \frac{1}{2} + \frac{P_d}{P_d^+} \cdot \frac{1}{2}, & P_d \ge 0. \\ \frac{1}{2} - \frac{P_d}{P_d^-} \cdot \frac{1}{2}, & P_d < 0. \end{cases} \tag{3}$$

Sensitivity homogenization is used in this paper to correct the correspondence between the value of the power demand and its rule of inference. However, since the FLC is not used in the EV mode, the BP's SoC also needs to be sensitively scaled to satisfy the boundaries of the $Mode_{FLC}$ working area. They are formulated mathematically through the relationship:

$$Input_2 = \frac{SoC - SoC_{min}}{SoC_{max} - SoC_{min}} \tag{4}$$

where $SoC_{min} = 0.2$ and $SoC_{max} = 0.5$ are the value of SoC boundary positions when the FLC is engaged.

2) Inference

The rule base, as shown in Table 2, determines the control outputs C and D with the inputs states A and B, by applying a 'if A and B then C and D' policy. A mathematic expression of the 'if A and B then C and D' policy is:

$$[C \quad D] = (A \times B) \circ R \tag{5}$$

where: 'A' denotes the fuzzy set of power demand; 'B' denotes the fuzzy set of SoC value; 'C' denotes the crisp value of the normalized motor rotational speed; 'D' denotes the crisp value of the normalized ISG power; and 'R' denotes the fuzzy relationship matrix indexed by the cross-product of 'A' and 'B'. The reasoning process is based on Eq. (5) with the Sugeno fuzzy set as described in the following table:

TABLE 2
FUZZY LOGIC BASED DECISION SYSTEM INFERENCE

Rule	Demand power	SoC value	Motor speed Ref.	ISG power Ref.
1	Low	Low	High	High
2	Medium	Low	Low	High
3	High	Low	Low	High
4	Low	Medium	High	Medium
5	Medium	Medium	Medium	Medium
6	High	Medium	Low	Medium
7	Low	High	High	Low
8	Medium	High	High	Low
9	High	High	Medium	Low

3) Defuzzification

In inference mechanism, the implied fuzzy sets are produced using the max–min composition. In defuzzification, these implied fuzzy sets are combined to provide a crisp value of controller outputs. There are several approaches to accomplish the defuzzification process and here the centroid of area method has been adopted because it is relatively simple and has good information preserving properties [6]. The final output is then expressed as the mean of the individual membership values weighted by the corresponding centroids as follows:

$$\left.\begin{aligned} Output_1 &= \frac{\sum_{i=1}^{n} Out1_i \cdot O_i}{\sum_{i=1}^{n} O_i}, \\ Output_2 &= \frac{\sum_{i=1}^{n} Out2_i \cdot O_i}{\sum_{i=1}^{n} O_i}, \end{aligned}\right\} \tag{6}$$

where, Out_i is the output of rule base i, and O_i is the centroid of the ith output MF. Based on Eq. (6), the rotational speed of the traction motor and the power ref. of the ISG can be calculated separately. From these outputs, the power distribution under the FLC mode is calculated as follows:

$$\left.\begin{aligned} n_{mot} &= Output_1 \cdot n_{mot}^*, \\ P_{gen} &= Output_2 \cdot P_{gen}^*, \\ T_{mot} &= T_d, \\ P_{ice} &= \begin{cases} P_d - n_{mot} \cdot T_{mot} - P_{gen}, & P_d \ge 0, \\ -P_{gen}, & P_d < 0, \end{cases} \end{aligned}\right\} \tag{7}$$

where, n_{mot}^* is the maximum speed of the traction motor, and P_{gen}^* is the maximum power of the ISG.

III. BACK-TO-BACK COMPETITIVE LEARNING MECHANISM

The back-to-back competitive learning mechanism (BCLM)

that is proposed in this research is shown in Fig. 2. The concept of the BCLM comprises two main modules: back-to-back learning; and competitive assessment. In the back-to-back learning module, two FLCs with the same structure were adopted. The first FLC is trained by an intelligent swarm optimizer, while the second serves the supervisory control system. In the competitive assessment module, there is an evaluator that competitively assesses the two controllers, and its assessment result decides both the control assignment to the supervisory controller system and the target of the optimizer. During the real-world driving, if better MF scalar parameters in the controller being trained are detected, both selectors (shown on Fig. 2) will be switched to their opposite side in order to concurrently exchange the current tasks of the two controllers. The controller being trained will take over the supervisory control system and the execution controller will hand over the optimization task. The main advantage of this parallel control structure is that it can ensure strong robustness and high efficiency of the supervisory control system whether before or after each update takes effect.

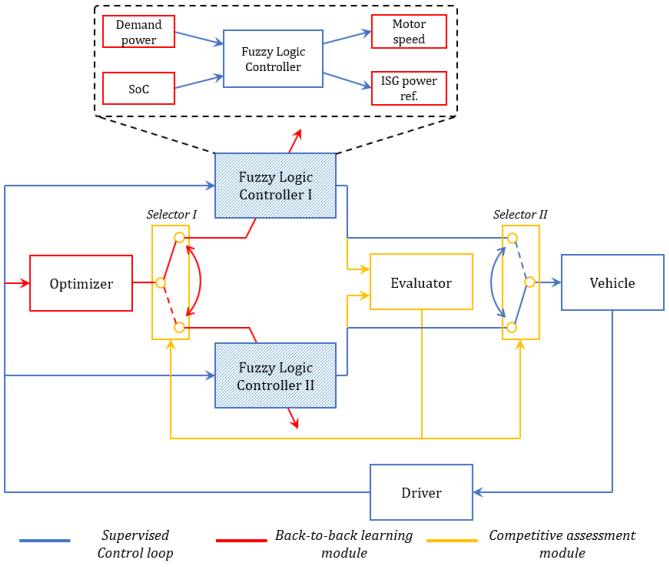

Fig. 2. Concept of back-to-back competitive learning mechanism

A. CAPSO-driven Back-to-back Learning

1) Search area and constraints

According to structure of the FLC, the boundary condition of the inputs and outputs are fixed at predetermined intervals. There is also no change to the fuzzy rules and the triangular MFs. The intelligent swarm optimizer is applied to each output. Here, the search variables in the multi-objective optimization problem are labelled in bold type shown in Fig. 3.

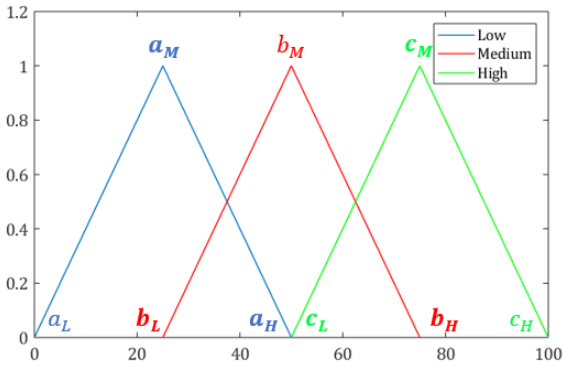

Fig. 3. Representation of triangular MFs

To simplify the implementation of optimization algorithms it is assumed here that the parameters a_M, b_L, a_H, c_L, b_H, and c_M are fixed for each input and output. In this way, 24 scalar parameters of the MFs need to be optimized, and the structure of the generic particle for each input and output is given by

$$|a_M \quad b_L \quad a_H \quad c_L \quad b_H \quad c_M| \tag{8}$$

Considering the structure of the FLC shown in Fig. 2, it is supposed that the six parameters to optimize each input and output must obey the following order criteria:

$$\left.\begin{array}{ll} a_L < a_M < a_H, & a_L < b_L < c_H, \\ a_L < a_H < b_M, & b_M < c_L < c_H, \\ b_M < b_H < c_H, & b_M < c_M < c_H. \end{array}\right\} \tag{9}$$

For each iteration of algorithm optimization, it is necessary to check the constraints in Eq. (9).

2) Cost functions and CAPSO algorithm

This paper considers two principal targets, the first is the overall liquid fuel consumption, and the second is the BP's SoC at the end of test. These cost functions are defined by:

$$\left.\begin{array}{l} J_1 = \dfrac{1}{\rho_{gaso}} \displaystyle\int \dot{m}_f(t)dt \\ J_2 = \dfrac{1}{SoC(t_{end})} \end{array}\right\} \tag{10}$$

where, ρ_{gaso} is the density of gasoline (0.77 g/ml); $\dot{m}_f$ is the fuel consumption mass rate (g/s); and t_{end} is the final time of the driving cycle.

To convert the multi-objective optimization problem into a single objective optimization enabling the swarm-based algorithm, in the present work, the multi-objective optimization is formulated by using the weighted sum method [34]. Therefore, the optimal energy-flow control problem with constrains is expressed as: minimize the overall cost function, J, given by

$$\min J = w \cdot \frac{J_1}{J_1^*} + (1-w) \cdot \frac{J_2}{J_2^*} \tag{11}$$

$$s.t. \begin{cases} SoC(k), & 0.8 \geq SoC(k) \geq 0.2 \\ n_{mot}(k), & n_{mot^*} \geq n_{mot}(k) \geq 0 \\ T_{mot}(k), & T_{mot^*} \geq T_{mot}(k) \geq -T_{mot^*} \\ P_{ICE}(k), & P_{ICE^*} \geq P_{ICE}(k) \geq 0 \\ P_{ISG}(k), & 0 \geq P_{ISG}(k) \geq -P_{ISG^*} \end{cases}$$

In Eq. (11), w is a weight coefficient; J_1^* and J_2^* are scaling constants for the cost functions, J_1 and J_2. The SoC contribution to the overall cost function ensures service life of the battery.

The CAPSO algorithm, which is an upgraded version of the accelerated particle swarm optimization (APSO) algorithm, is a computational algorithm inspired by animal swarms such as ant colonies, bird flocks, fish schools, and other biological phenomena [35]. The standard APSO usually keeps the attraction parameters as a fixed value [36]; however, the solutions still change slightly as the optima are approached. In the chaos-enhanced algorithm, a dynamic attraction parameter in each iteration is used to create some 'accidents', which help the particles to jump out of any convergence to a local optimum proved by [37], [38]. For the CAPSO, the particle's position updates with the following equation:

$$x^{(i+1,j)} = (1-\beta)\cdot x^{(i,j)} + \beta \cdot g^{(i,*)} + \alpha^{(i)} \cdot r^{(i,j)} \quad (12)$$

In Eq. (12), $g^{(i,*)}$ is the best position in the ith iteration, β is the attraction parameter of CAPSO, α is the convergence parameters of CAPSO, and r is a $U[0,1]$ random variable. Here, α and β are updated in each iteration via:

$$\left.\begin{aligned} \alpha^{(i)} &= \alpha^{(0)} \cdot \gamma^{i}, \\ \beta^{(i+1)} &= a \cdot \beta^{(i)} \cdot (1-\beta^{(i)}), \end{aligned}\right\} \quad (13)$$

where, the settings, $\alpha^{(0)} = 0.9$ and $\gamma = 0.95$, were chosen; and the attraction parameter is mapped by the logistic map [35], in which the initial values $\beta^{(1)} = 0.6$ and $a = 4$ are used. When $\beta \to 0$ in any step, the algorithm may lead to slow changes. After the convergence has been achieved, the algorithm ends the main iteration and outputs the best position at the end iteration $g_{\max\ \_iter,*}$ as the global optimal solution.

B. Fuel-prioritized Competitive Assessment

1) Observation window for assessment

To evaluate the fuel-saving performance for both FLCs with back-to-back learning, a short-term moving window H is introduced. The observation window ensures that the competition between both controllers is fair and that the reference driving profiles for CAPSO-driven back-to-back learning are equal.

Short-term speed and acceleration profiles are expected to be strongly influenced by variables with fast dynamics such as traffic congestion and driving style. This paper examines the impact of the length of observation windows in the fuel-prioritized competitive assessment on the vehicle's fuel consumption. Different lengths of short-term windows are studied in the control system driven by the proposed mechanism.

2) Competitive assessment procedure

Figure 4 sets out the competitive assessment procedure for electing the controller with the better fuel-saving performance. In each time-step, the optimizer calls the CAPSO algorithm to search the global best solution for the controller being trained based on the short-term driving profile restricted by the observation window. The best scalar parameters for the MFs are used in the controller being trained then the evaluator calculates the fuel-saving performance of both controllers.

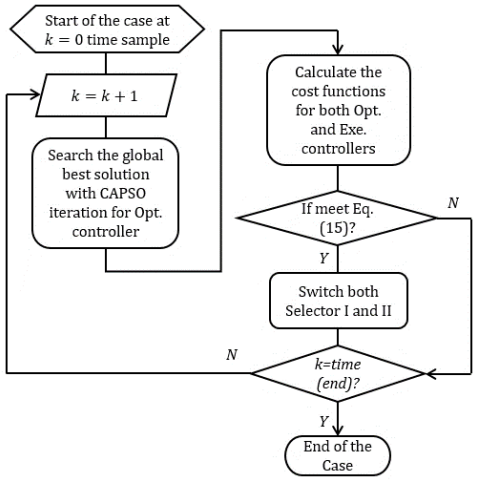

Fig. 4. Flowchart of competitive assessment procedure

Considering the impact of length of observation windows on the vehicle's fuel consumption, the cost function from Eq. (11) for each controller is modified as follows:

$$\left.\begin{aligned} csn_{exe} &= w \cdot \frac{J_1'}{H \cdot J_1^*} + (1-w) \cdot \left(\frac{J_2'}{H \cdot J_2^*}\right)^2, \\ csn_{opt} &= w \cdot \frac{J_1''}{H \cdot J_1^*} + (1-w) \cdot \left(\frac{J_2''}{H \cdot J_2^*}\right)^2, \end{aligned}\right\} \quad (14)$$

where, H is length of the observation window; csn_{exe} and csn_{opt} are, respectively, the cost functions of the execution controller and the controller being trained; J_1' and J_2' are the evaluation objects for the execution controller; and J_1'' and J_2'' are the evaluation objects for the controller being trained. It should be noted that the introduced observation window would increase the sensitivity to the change of J_1 and reduces that for J_2. To ensure sufficient service life of the battery, the order of penalty J_2 should be increased when SoC value is low. Fig. 5 investigates the average value of cost function with different orders of penalty during real world driving with the initial SoC value of 0.2. The cost functions of both objectives are scaled to the same range of [0,1] with w fixed at 0.5 in Eq. (14). Compared to other investigated orders, the quadratic penalty J_2 gives the only positive differential related to J_1.

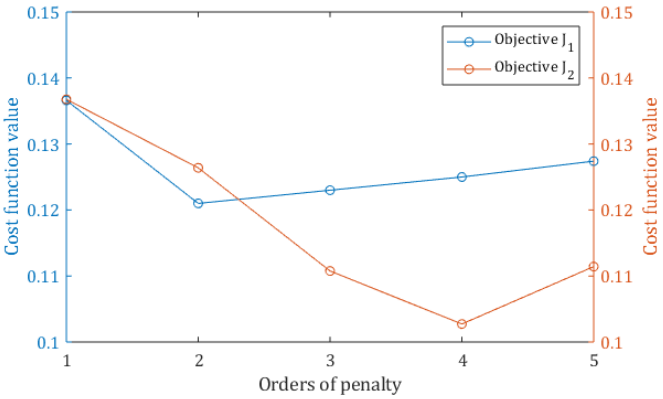

Fig. 5. Statistical results of cost function with different orders' penalty

In real time driving, cost functions of the execution controller are considered as a learning target to motivate another. At each

time-step, the BCLM will calculate the cost functions of both controllers. If the current state meets the following conditions:

$$\left.\begin{aligned} csn_{opt}(k) - csn_{exe}(k) < 0, \text{and} \\ \frac{csn_{opt}(k) - csn_{exe}(k)}{csn_{opt}(k-1) - csn_{exe}(k-1)} < 1. \end{aligned}\right\} \quad (15)$$

where, errors and its derivatives between two cost function values as the main factors in this paper affect the final decision. If $csn_{opt}(k-1) - csn_{exe}(k-1) = 0$, then only the first condition of Eq. (15) needs to be satisfied and the proposed mechanism takes action to switch both selectors to the other side, exchanging the current tasks and roles between the two controllers. Otherwise, the two controllers will continue to operate their current tasks and the mechanism will explore the MF scalar parameters searching for better fuel-saving performance for the next time step.

IV. Testing and Validation Set-up

A. Real-world Driving Cycles

As the goal of this work is to develop a supervisory control system that learns and adapts to human driving style the previously discussed HEV model was implemented in a driving simulator. Five human drivers were invited as experimental subjects to participate in 8000 seconds of real-world driving. The road map model used was a mixture of highway and local roads with traffic, multiple stop signs, traffic lights, and speed limit changes: it was provided by IPG CarMaker and is shown in Fig. 6. The human driver was instructed to follow the speed limits, stop signs, traffic lights, and other traffic regulations. The specification of the real-world driving cycle is listed in Table 3.

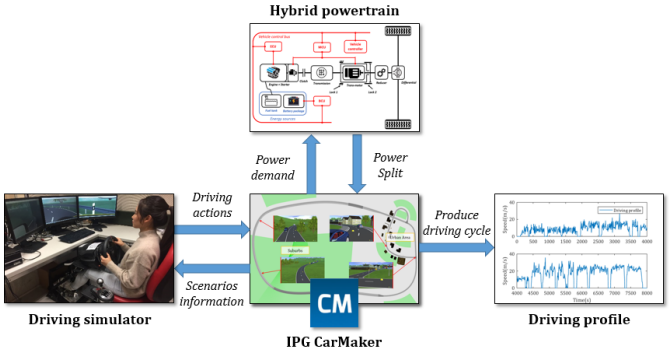

Fig. 6. Data collection of driving profiles

TABLE 3
SPECIFICATION OF REAL-WORLD DRIVING CYCLE

Human driver	Traffic type	Driving time(s)	Driving distance(km)
A	Urban	1880	11.6
B	Urban	1590	17.8
C	Urban	940	8.1
D	Highway	1350	22.5
E	Highway	2240	40.0

B. Hardware-in-the-loop Experiment

The work was carried out using the industry standard real-time testing equipment sourced from the ETAS Group [39]. The configuration of the HiL testing system is shown in Fig. 7. Firstly, the HEV model and its FL-based control system were compiled as MATLAB® code. Secondly, through the host PC, they were imported into the integration platform, which is the user interface through which the HiL system is configured, in preparation for creating signal paths between the models and the hardware, and generating code for the LABCAR simulation target LABCAR-RTPC. Thirdly, the whole vehicle system was downloaded to the DESK-LABCAR using the ETAS experimental environment (EE) via Ethernet protocol. In the experiment, vehicle performance was entirely supervised by the ETAS EE in the host PC. From the recorded results, the average computational time for CAPSO algorithm to complete an iterative convergence is 0.225 seconds so the computing resource still has a surplus for the current version given the fact that its capacity will continue to increase. As indicated by Moore's Law, it is anticipated the BCLM can perform on the actual on-board controller of HEVs for real-time energy saving.

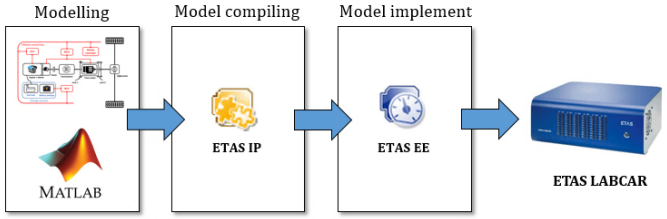

Fig. 7. Hardware-in-the-loop testing system

V. Results and Discussion

A. Back-to-back Learning Performance

In this section, the evaluation of the back-to-back learning is presented in two parts as a performance comparison of optimization algorithms and the MF evolution process. Fig. 8 shows the cost function values achieved by the different swarm-based optimization algorithms averaged over 30 runs for 15 iterations.

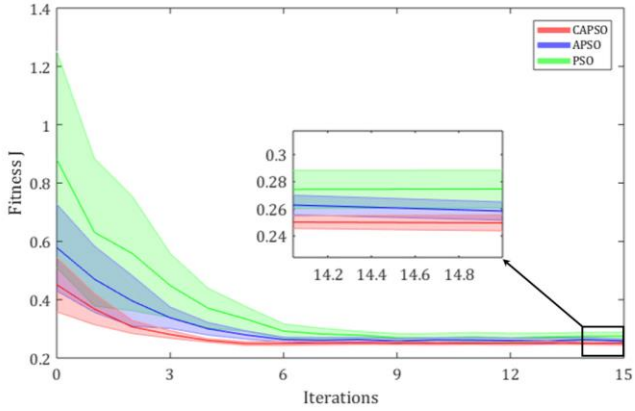

Fig. 8. Performance comparison of optimization algorithms

In each run: 20 particles for each variable in the swarm-based algorithms were initialized randomly; the weight coefficient of the cost function was set to $w = 0.7$; and the termination criterion was 15 iterations. From the results, all swarm-based algorithms realize fitness function convergence within 15 iterations. Especially at the fifth iteration, the CAPSO algorithm has reached the best global solutions while others are still in convergence. Therefore, the CAPSO algorithm enhanced by the chaos mapping strategy is more ambitious in expanding the exploration area for the global solution search.

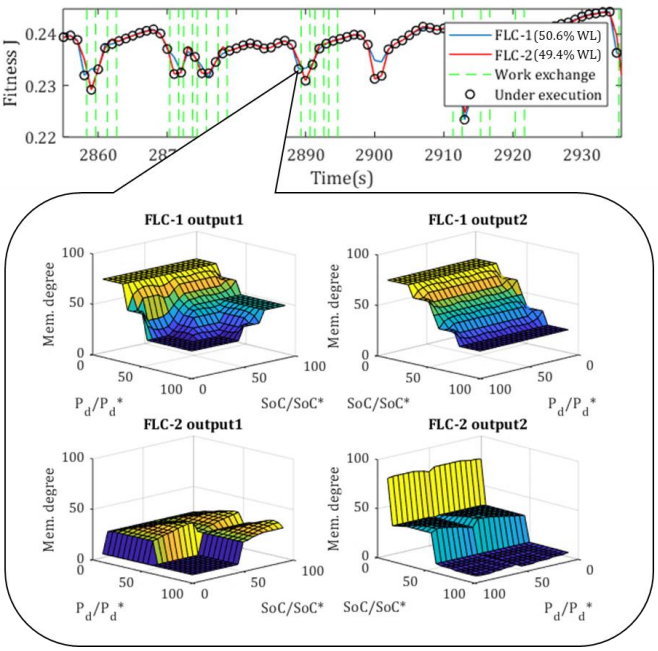

Fig.9. Real-time performance of two FLCs boosted by the BCLM

Figure 9 shows a fragment of real-time performance of two FLCs, wherein the green dotted line indicates the timing of two controllers' work exchange and the black circle indicates the fitness in the execution controller of HEV systems. From the results of the top subfigure, two controllers are alternately updated by the BCLM and their work exchanges frequently at protruding spikes, which are caused by the dramatic changing in human driving behaviours. Although the working time and training time between two controllers cannot exactly equal in each optimization fragment, the BCLM can schedule them in relative balance to make both controllers have fair workloads (50.6% and 49.4%) during the long-term driving. The bottom subfigure dissects output surface evolution process between two FLCs at the 2889th seconds. It can be seen that the BCLM will abandon a relatively smooth output surface used for most driving scenarios and replace to an aggressive one for targeting higher fuel economy.

B. Vehicle Performance Comparison

In Fig. 10, the FL-based supervisory control system with the proposed mechanism is further compared with the conventional FL-based one during real-world driving. The fuel consumption under the FL-based control system with the proposed mechanism is significantly lower than the conventional one, while maintaining the higher SoC value. Boosted by the BCLM, the ICE initially tends to compensate for the total power demand to avoid the potential danger of a rapid drop in the BP's SoC. The ISG maintains a higher workload compared to that supervised by the conventional FL-based control system.

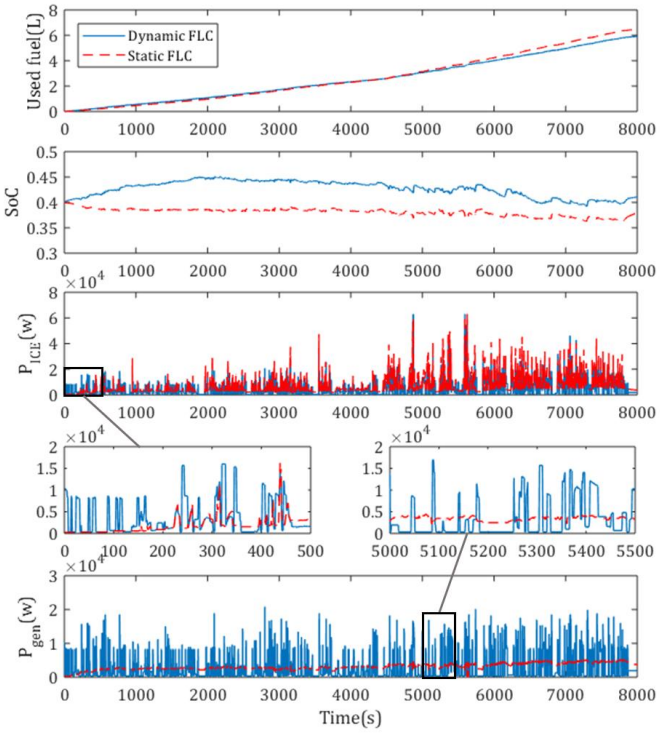

Fig. 10. Vehicle performance comparisons at initial SoC=0.4

The vehicle performance with different control strategies is summarized in Table 4. An analogous result can also be observed for initial SoCs of 0.5 and 0.3. The classic rule-based control strategies of charge depleting (CD) and charge sustaining (CS) were considered and used as a baseline for comparison with the FL-based strategies. As the decrease of initial SoC values, the space for freely distributing energy is narrowed. Compared to the CD/CS strategy, the static FL-based system after offline optimization can adaptively adjust energy distribution in the narrow SoC range but its improvement is not significant. Relatively, the dynamic FL-based system with the help of the BCLM always selects a controller with better cost-function value in real time to counter driving scenario change. The result shows the improved system has the lowest fuel consumption while maintaining the highest SoC value, compared to the performance of others.

TABLE 4
THE VEHICLE PERFORMANCE WITH DIFFERENT CONTROL STRATEGIES

Control strategy	Initial SoC	Final SoC	Used Fuel (L)	Saving (%)
CD/CS	0.5	0.353	6.41	-
Static FLC	0.5	0.379	6.24	2.7%
Dynamic FLC	0.5	0.408	5.44	15.1%
CD/CS	0.4	0.351	6.63	
Static FLC	0.4	0.379	6.48	2.3%
Dynamic FLC	0.4	0.412	5.88	11.3%
CD/CS	0.3	0.352	6.89	-
Static FLC	0.3	0.379	6.75	2.0%
Dynamic FLC	0.3	0.408	6.26	9.14%

C. Horizon Sensitivity Analysis

As discussed earlier, the observation window was introduced into the BCLM to regulate the learning range of the optimizer. In this section, the impact of the length of the observation

window on the input-output signals of the controller is investigated, following which the sensitivity of the length of the observation window to the average applicable time for one set of MFs is analysed.

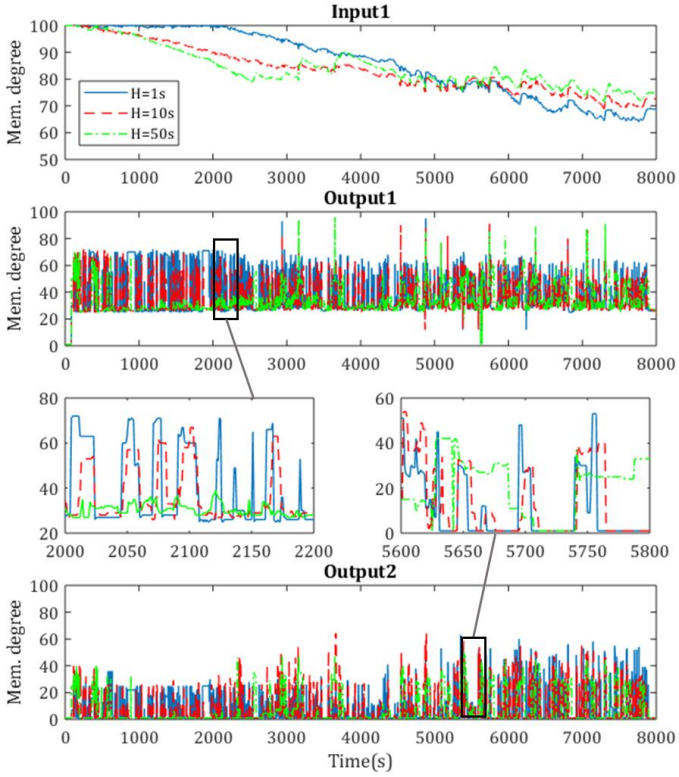

Fig. 11. The signal comparison over observation window lengths

Fig. 11 presents the signal comparison with different lengths of the observation window ($H = 1\,\text{s}/10\,\text{s}/50\,\text{s}$) when the initial SoC=0.5. As the length of the observation window increases, the early-cycle power provided by the motor rises, and the number of occurrences of peak trans-motor rotational speed increases gradually. For the improved control system, the aggressive braking power can be better absorbed when the observation window, H, is 50 s than when it is 1 s or 10 s. This leads to the signal of SoC value dropping fast at an early stage, after which the signal is stable within a small range of oscillation.

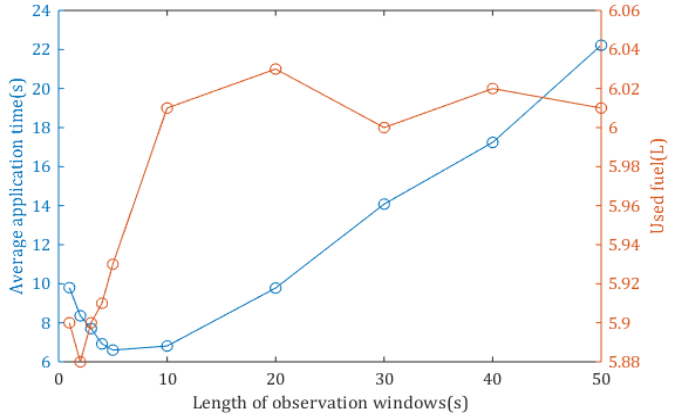

Fig. 12. Computational efficiency over backward horizons

Figure 12 shows the average application time and the fuel consumption over backward horizons, wherein the tests with the initial SoC=0.4 in each scenario were each repeated 10 times. As the length of observation windows shorten (< 5 s), the rules in the fuzzy inference to be called lessen, and involved scalar parameters of corresponding MFs to be optimized are relatively limited and fixed. Therefore, optimized scalar parameters have longer average application time. The average application time troughs at 6.60 seconds at which the length of observation windows is 5 seconds. After that, as the length of observation windows increases (> 5 s), the rules in the fuzzy inference to be called increases and even some single rules are called multiple times. It results in that involved scalar parameters of corresponding MFs to be optimized need to balance under multiple scenarios. Therefore, optimized scalar parameters with stronger adaptability can handle more driving scenarios thereby average application time is longer. The lowest fuel consumption (on the second y-axis) occurs when the length of observation windows is 2 seconds. As the most suitable observation duration of driving events, this result is consistent with the view of Clara Marina and Cao [40]. After which the fuel consumption rises rapidly to 6.03 L ($at\ H = 20$ s) then remains at a high level on further increase of H.

VI. Conclusions

This paper proposes a back-to-back competitive learning mechanism for a FL-based supervisory control system to improve the fuel-saving efficiency of HEV energy management. The back-to-back learning performance is evaluated and compared with that optimized by other swarm-based algorithms. The contributions drawn from the investigation are as follows:

1) The proposed mechanism has demonstrated abilities to adapt to the change of driving behaviours and to ensure the effectiveness of the FL-based control system by real-time MF parameter updates (957 times) in the case study.
2) Under different initial SoC conditions ($SoC = 0.3/0.4/0.5$), the FL-based control system driven by the proposed mechanism can significantly improve the fuel consumption when compared to CD/CS and conventional FL-based control strategies.
3) The improved FL-based control system reduces fuel consumption over the testing real-world cycle, at least 9% from CD/CS-based and at least 7% from conventional FL-based systems.
4) Comparing the various size of observation windows from 1 to 50 s, the 2-second observation window appears to be the best for learning from backward horizons achieving the lowest fuel consumption of 5.88 litres/100 km.

References

[1] Y. Wu *et al.*, 'Energy consumption and CO 2 emission impacts of vehicle electrification in three developed regions of China', vol. 48, pp. 537–550, 2012.
[2] F. Zhang, X. Hu, R. Langari, and D. Cao, 'Energy management strategies of connected HEVs and PHEVs : Recent progress and outlook', vol. 73, pp. 235–256, 2019.
[3] M. F. M. Sabri, K. A. Danapalasingam, and M. F. Rahmat, 'A review

on hybrid electric vehicles architecture and energy management strategies', *Renewable and Sustainable Energy Reviews*, vol. 53, pp. 1433–1442, 2016.

[4] G. Kalghatgi, 'Is it really the end of internal combustion engines and petroleum in transport ?', *Applied Energy*, vol. 225, no. May, pp. 965–974, 2018.

[5] Y. Huang, H. Wang, A. Khajepour, H. He, and J. Ji, 'Model predictive control power management strategies for HEVs : A review', *Journal of Power Sources*, vol. 341, pp. 91–106, 2017.

[6] L. A. H. Zad, 'A fuzzy-algorithmic approach to the definition of complex or imprecise concepts', *International Journal of Man-Machine Studies*, pp. 249–291, 1976.

[7] M. Haghighat and M. Abdel-mottaleb, 'Discriminant Correlation Analysis : Real-Time Feature Level Fusion for Multimodal Biometric Recognition', *IEEE Transactions on Information Forensics and Security*, vol. 11, no. 9, pp. 1984–1996, 2016.

[8] C. M. Martinez, M. Heucke, F. Wang, B. Gao, and D. Cao, 'Driving Style Recognition for Intelligent Vehicle Control and Advanced Driver Assistance : A Survey', *IEEE Transactions on Intelligent Transportation Systems*, vol. 19, no. 3, pp. 666–676, 2018.

[9] S. Zhang and R. Xiong, 'Adaptive energy management of a plug-in hybrid electric vehicle based on driving pattern recognition and dynamic programming', *Applied Energy*, vol. 155, pp. 68–78, 2015.

[10] J. Jing, D. Filev, A. Kurt, E. Özatay, J. Michelini, and Ü. Özgüner, 'Vehicle Speed Prediction using a Cooperative Method of Fuzzy Markov Model and Auto-regressive Model', in *Intelligent Vehicles Symposium (IV), 2017 IEEE*, 2017, no. Iv, pp. 881–886.

[11] D. P. Filev and I. Kolmanovsky, 'Generalized Markov Models for Real-Time Modeling of Continuous Systems', *IEEE TRANSACTIONS ON FUZZY SYSTEMS*, vol. 22, no. 4, pp. 983–998, 2014.

[12] J. Li *et al.*, 'Dual-loop online intelligent programming for driver-oriented predict energy management of plug-in hybrid electric vehicles', *Applied Energy*, vol. 253, no. November, p. 113617, 2019.

[13] X. Li, Z. Liu, and K. Leung, 'Detection of vehicles from traffic scenes using fuzzy integrals', *Pattern Recognition*, vol. 35, pp. 967–980, 2002.

[14] V. Milanés *et al.*, 'Intelligent automatic overtaking system using vision for vehicle detection', *Expert Systems with Applications*, vol. 39, pp. 3362–3373, 2012.

[15] A. A. Ferreira, J. A. Pomilio, S. Member, G. Spiazzi, and L. D. A. Silva, 'Energy Management Fuzzy Logic Supervisory for Electric Vehicle Power Supplies System', *IEEE TRANSACTIONS ON POWER ELECTRONICS*, vol. 23, no. 1, pp. 107–115, 2008.

[16] H. Khayyam and A. Bab-hadiashar, 'Adaptive intelligent energy management system of plug-in hybrid electric vehicle', *Energy*, vol. 69, pp. 319–335, 2014.

[17] R. Zhang, J. Tao, and H. Zhou, 'Fuzzy Optimal Energy Management for Fuel Cell and Supercapacitor Systems Using Neural Network', *IEEE Transactions on Fuzzy Systems*, vol. 27, no. 1, pp. 45–57, 2019.

[18] J. Solano, R. I. John, D. Hissel, and M. Péra, 'A survey-based type-2 fuzzy logic system for energy management in hybrid electrical vehicles', *Information Sciences*, vol. 190, pp. 192–207, 2012.

[19] F. Harel, D. Hissel, R. I. John, and M. Amiet, 'Experimental validation of a type-2 fuzzy logic controller for energy management in hybrid electrical vehicles', *Engineering Applications of Artificial Intelligence*, vol. 26, pp. 1772–1779, 2013.

[20] A. Kheirandish, F. Motlagh, N. Shafiabady, M. Dahari, A. Khairi, and A. Wahab, 'Dynamic fuzzy cognitive network approach for modelling and control of PEM fuel cell for power electric bicycle system', *Applied Energy*, vol. 202, pp. 20–31, 2017.

[21] H. Tian, S. E. Li, X. Wang, Y. Huang, and G. Tian, 'Data-driven hierarchical control for online energy management of plug-in hybrid electric city bus', *Energy*, vol. 142, pp. 55–67, 2018.

[22] D. Zhou, A. Al-durra, F. Gao, A. Ravey, I. Matraji, and M. Godoy, 'Online energy management strategy of fuel cell hybrid electric vehicles based on data fusion approach', vol. 366, pp. 278–291, 2017.

[23] M. Collotta, G. Pau, and V. Maniscalco, 'A Fuzzy Logic Approach by Using Particle Swarm Optimization for Effective Energy Management in IWSNs', vol. 64, no. 12, pp. 9496–9506, 2017.

[24] C. Caraveo, F. Valdez, and O. Castillo, 'Optimization of fuzzy controller design using a new bee colony algorithm with fuzzy dynamic parameter adaptation', *Applied Soft Computing Journal*, vol. 43, pp. 131–142, 2016.

[25] I. V Kolmanovsky, 'Game Theory Controller for Hybrid Electric Vehicles', vol. 22, no. 2, pp. 652–663, 2014.

[26] C. M. Martinez, X. Hu, D. Cao, E. Velenis, B. Gao, and M. Wellers, 'Energy Management in Plug-in Hybrid Electric Vehicles : Recent Progress and a Connected Vehicles Perspective', *IEEE TRANSACTIONS ON VEHICULAR TECHNOLOGY*, vol. 66, no. 6, pp. 4534–4549, 2017.

[27] T. Liu, X. Hu, S. E. Li, and D. Cao, 'Reinforcement Learning Optimized Look-Ahead Energy Management of a Parallel Hybrid Electric Vehicle', *IEEE/ASME TRANSACTIONS ON MECHATRONICS*, vol. 22, no. 4, pp. 1497–1507, 2017.

[28] V. Mnih *et al.*, 'Human-level control through deep reinforcement learning', *Nature*, vol. 218, no. 7540, p. 529, 2015.

[29] Y. Wu, H. Tan, J. Peng, H. Zhang, and H. He, 'Deep reinforcement learning of energy management with continuous control strategy and tra ffi c information for a series-parallel plug-in hybrid electric bus', *Applied Energy*, vol. 247, no. March, pp. 454–466, 2019.

[30] S. Ahmadi, S. M. T. Bathaee, and A. H. Hosseinpour, 'Improving fuel economy and performance of a fuel-cell hybrid electric vehicle (fuel-cell , battery , and ultra-capacitor) using optimized energy management strategy', *Energy Conversion and Management*, vol. 160, no. December 2017, pp. 74–84, 2018.

[31] F. Silva and C. R. C. Press, 'Electric power systems (review of "Modern Electric, Hybrid Electric, and Fuel Cell Vehicles: Fundamentals, Theory, and Design, Second Edition ; Ehsani, Y.G. and Emadi, A.; 2010) [Book News]', *IEEE Industrial Electronics Magazine*, vol. 4, no. March, p. 75, 2010.

[32] X. Zeng, J. Wang, and S. Member, 'A Stochastic Driver Pedal Behavior Model Incorporating Road Information', *IEEE TRANSACTIONS ON HUMAN-MACHINE SYSTEMS*, vol. 47, no. 5, pp. 614–624, 2017.

[33] M. Ehsani, Y. Gao, S. Longo, and K. Ebrahimi, *Modern electric, hybrid electric, and fuel cell vehicles*. CRC press, 2018.

[34] R. T. Marler and J. S. Arora, 'The weighted sum method for multi-objective optimization : new insights', *Structural and multidisciplinary optimization*, vol. 41, no. 6, pp. 853–862, 2010.

[35] A. Hossein, G. Jin, X. Yang, and S. Talatahari, 'Chaos-enhanced accelerated particle swarm optimization', *Communications in Nonlinear Science and Numerical Simulation*, vol. 18, no. 2, pp. 327–340, 2013.

[36] J. Kennedy, 'Particle swarm optimization', in *Encyclopedia of machine learning*, Springer, pp. 760–766.

[37] Q. Zhou, W. Zhang, S. Cash, O. Olatunbosun, H. Xu, and G. Lu, 'Intelligent sizing of a series hybrid electric power-train system based on Chaos-enhanced accelerated particle swarm optimization', *Applied Energy*, vol. 189, pp. 588–601, 2017.

[38] Q. Zhou, Y. Zhang, Z. Li, J. Li, H. Xu, and O. Olatunbosun, 'Cyber-Physical Energy-Saving Control for Hybrid Aircraft-Towing Tractor Based on Online', *IEEE TRANSACTIONS ON INDUSTRIAL INFORMATICS*, vol. 14, no. 9, pp. 4149–4158, 2018.

[39] 'ETAS products', *ETAS Group*, 2018. [Online]. Available: https://www.etas.com/en/index.php?langS=true.

[40] C. M. Martinez and D. Cao, *IHorizon-Enabled Energy Management for Electrified Vehicles*. Butterworth-Heinemann, 2018.

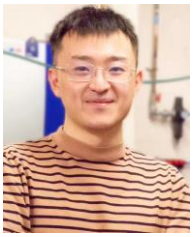

Ji Li received the B.S. degree (Hons) in vehicle engineering from the Chongqing University of Technology, Chongqing, China, in 2015. He is currently working toward the Ph.D. degree at the Intelligent Vehicle System and Control Team, University of Birmingham, Birmingham, U.K. His current research interests fuzzy mathematics, deep reinforcement learning, Meta-heuristic algorithms and development of driving behavior recognition, and vehicle intelligent systems optimization.

Quan Zhou (M'17) received the B.Eng. and M.Res. degrees (Hons) in vehicle engineering from Wuhan University of Technology, Wuhan, China, in 2012 and 2015, respectively. He is currently a scholarship-funded Ph.D. Researcher at the Intelligent Vehicle System and Control Team, Vehicle and Engine Technology Research Centre, University of Birmingham, Birmingham, U.K. His research interests include vehicle system modeling, HEV/EV design optimization, optimal control, and artificial intelligence for future HEVs and CAVs.

Huw Williams is a UK-based business consultant offering a wide range of skills to all types of businesses. He is a professional mathematician with excellent skills in Lean, Six Sigma, Engineering Physics and Statistics. Huw has over 20 years experience in the automotive industry; he graduated from the University of Oxford in 1978 with a mathematics degree and went on to take a PhD in theoretical mechanics at the University of East Anglia. His early career comprised research work on the mechanical properties of ice for the US Army followed by a spell as a mathematics lecturer at Edinburgh's Heriot-Watt University where he researched in theoretical mechanics. Huw joined Jaguar Cars in 1986 where he worked in research and development applying mathematical modelling techniques to all aspects of vehicle technology. He also developed statistical skills through TQM in the 1980's culminating in his accreditation as Ford's top-scoring Master Black Belt in 2005.

Hongming Xu received the Ph.D. degree in mechanical engineering from Imperial College London, London, U.K. He is a Professor of Energy and Automotive Engineering at the University of Birmingham, Birmingham, U.K., and the Head of Vehicle and Engine Technology Research Centre. He has six years of industrial experience with Jaguar Land Rover and Premier Automotive Group of Ford. He has authored and co-authored more than 300 journal and conference publications on advanced vehicle powertrain systems involving both experimental and modeling studies.

Prof. Xu was a member of the Ford HCCI Global Steering Committee, a Project Manager and Technical Leader of U.K. Foresight Vehicle LINK projects CHARGE and CHASE from 2002 to 2007. He is a Fellow of SAE International and IMechE.